Monitoring Drug-Target Interactions through Target Engagement-Mediated Amplification on Arrays and in situ

Rasel Al-Amin (drrasel.alamin@gmail.com)
Uppsala University https://orcid.org/0000-0002-0762-9034

Lars Johansson
Department of Medical Biochemistry and Biophysics, Chemical Biology Consortium Sweden (CBCS), Science for Life Laboratory, Karolinska Institutet

Eldar Abdurakhmanov
Department of Chemistry-BMC, Science for Life Laboratory, Uppsala University

Nils Landegren
Center for Molecular Medicine, Department of Medicine (Solna), Science for Life Laboratory, Karolinska Institutet. Department of Medical Sciences, Uppsala University.

Liza Löf
Department of Immunology, Genetics and Pathology, Science for Life Laboratory

Linda Arngården
Department of Medical Sciences, Uppsala University

Andries Blokzijl
Department of Immunology, Genetics and Pathology, Science for Life Laboratory

Richard Svensson
Department of Pharmacy, Uppsala University Drug Optimization and Pharmaceutical Profiling (UDOPP), Science for Life Laboratory, Uppsala University

Maria Hammond
Department of Immunology, Genetics and Pathology, Science for Life Laboratory

Peter Lönn
Department of Immunology, Genetics and Pathology, Science for Life Laboratory
https://orcid.org/0000-0002-2405-9010

Johannes Haybaeck
Institute of Pathology, Neuropathology and Molecular Pathology, Medical University of Innsbruck. Diagnostic and Research Institute of Pathology, Medical University of Graz

Masood Kamali-Moghaddam
Uppsala University https://orcid.org/0000-0002-1303-2218

Annika Jensen

Department of Medical Biochemistry and Biophysics, Chemical Biology Consortium Sweden (CBCS), Science for Life Laboratory, Karolinska Institutet

U Helena Danielson

Uppsala University https://orcid.org/0000-0003-2728-0340

Per Artursson

Uppsala University https://orcid.org/0000-0002-3708-7395

Thomas Lundbäck

Department of Medical Biochemistry and Biophysics, Chemical Biology Consortium Sweden (CBCS), Science for Life Laboratory, Karolinska Institutet

Ulf Landegren

Uppsala University https://orcid.org/0000-0002-7820-1000

Article

Keywords:

Posted Date: December 6th, 2021

DOI: https://doi.org/10.21203/rs.3.rs-1109577/v1

Monitoring Drug-Target Interactions through Target Engagement-Mediated Amplification on Arrays and *in situ*

Rasel A. Al-Amin[*,1], Lars Johansson[2], Eldar Abdurakhmanov[3], Nils Landegren[4,5], Liza Löf[1,9], Linda Arngården[5,9], Andries Blokzijl[1], Richard Svensson[6], Maria Hammond[1,10], Peter Lönn[1,10], Johannes Haybaeck[7,8,10], Masood Kamali-Moghaddam[1,10], Annika Jenmalm Jensen[2,10], Helena Danielson[3,10], Per Artursson[6], Thomas Lundbäck[2], Ulf Landegren[*,1]

[1]Department of Immunology, Genetics and Pathology, Science for Life Laboratory, Uppsala University, Sweden.
[2]Department of Medical Biochemistry and Biophysics, Chemical Biology Consortium Sweden (CBCS), Science for Life Laboratory, Karolinska Institutet, Sweden.
[3]Department of Chemistry-BMC, Science for Life Laboratory, Uppsala University, Sweden.
[4]Center for Molecular Medicine, Department of Medicine (Solna), Science for Life Laboratory, Karolinska Institutet, Sweden.
[5]Department of Medical Sciences, Uppsala University, Sweden.
[6]Department of Pharmacy, Uppsala University Drug Optimization and Pharmaceutical Profiling (UDOPP), Science for Life Laboratory, Uppsala University, Sweden.
[7]Institute of Pathology, Neuropathology and Molecular Pathology, Medical University of Innsbruck, Austria.
[8]Diagnostic and Research Institute of Pathology, Medical University of Graz, Austria.

Authors [9]L.A. and L.L. contributed equally. [10]These (M.H., J.H., P.L., M.K.-M., A.J.J. and H.D.) authors contributed equally.

[*]Email**:** rasel.al-amin@igp.uu.se; ulf.landegren@igp.uu.se

Drugs are designed to bind their target proteins in physiologically relevant tissues and organs to modulate biological functions and elicit desirable clinical outcomes. Information about target engagement at cellular and subcellular resolution is therefore critical for guiding compound optimization in drug discovery, and for probing resistance mechanisms to targeted therapies in clinical samples. We describe a target engagement-mediated amplification (TEMA) technology, where oligonucleotide-conjugated drugs are used to visualize and measure target engagement *in situ*, amplified via rolling-circle replication of circularized oligonucleotide probes. We illustrate the TEMA technique using dasatinib and gefitinib, two kinase inhibitors with distinct selectivity profiles. *In vitro* binding by dasatinib probe to arrays of displayed proteins accurately reproduced known selectivity profiles, while their differential binding to a panel of fixed adherent cells agreed with expectations from expression profiles of the cells. These findings were corroborated by competition experiments using kinase inhibitors with overlapping and non-overlapping target specificities, and translated to pathology tissue sections. We also introduce a proximity ligation variant of TEMA in which these drug-DNA conjugates are combined with antibody-DNA conjugates to selectively investigate binding to specific target proteins of interest. This form of the assay serves to improve resolution of binding to on- and off-target proteins. In conclusion, TEMA has the potential to aid in drug development and clinical routine by conferring valuable insights in drug-target interactions at spatial resolution in protein arrays, cells and tissues.

Introduction

Analysis of target binding by small drug molecules is critical in drug discovery as it ties interactions with intended targets and unwanted off-targets to clinically relevant pharmacology[1-4]. Despite significant methodological advances in assessment of such target engagement among cells and tissues[5,6], preclinical testing often fails to fully capture human responses to drugs, leading to attrition in clinical trials because of insufficient efficacy or compromised safety[7,8].

Protein kinases are a frequently targeted component of the druggable proteome, and the second largest target protein family for drug discovery[9-11]. Kinases are involved in intracellular signal transduction in processes such as cellular growth, differentiation, and apoptosis in the course of normal cellular functions, and they play crucial roles in human diseases, notably in cancer[12,13]. Key structural elements of the active sites are conserved across some 518 human kinases, and unwanted effects on off-target kinases is a common challenge in developing kinase inhibitors[14,15]. In keeping with this notion, there is a broad repertoire of techniques available for kinase selectivity profiling[16-19], many of which are based on inhibition of recombinant kinase activity or competition assays based on immobilized or labelled tracer molecules. Kinase target engagement can also be assessed in live cells using fluorescence or bioluminescence resonance energy transfer (FRET or BRET, respectively), provided both the drug molecule and its kinase targets can be suitably modified[20,21]. Given the availability of exquisitely selective tracers such measurements can also provide spatial resolution both *in vitro* and *in vivo* using *e.g.* fluorescence lifetime imaging microscopy (FLIM) [22,23]. While the above mentioned approaches are generally applied to one kinase at the time, the field also frequently adopts chemoproteomics approaches, where *e.g.* modified nucleotide analogs or activity-based probes are employed for a more complete understanding of kinase selectivity in lysed cells and tissues[24-26].

Target engagement can also be measured in live cells without or with only minimal prior modification of either interaction partner. One such technique is the cellular thermal shift assay (CETSA), which measures underivatized drug binding to endogenous proteins in live cells and tissues by monitoring thermal stabilization of target proteins[27-30]. While significant progress has been made to allow CETSA measurements in tissues of treated animals, whole blood samples, and fine needle aspirates[31,34], such measurements can only be achieved with single cell resolution under special circumstances[31-34]. Instead, localized measurement remain dependent on the use of radiolabeled drugs in low resolution imaging by positron emission tomography (PET) or the combined use of fluorescent tracers and fusion proteins to generate NanoBRET signals[6,35-36]. These limitations illustrate the need for new approaches to measure physiologically relevant target engagement, and in particular for techniques that can provide both cellular and target protein resolution. Ideally such methods would allow probing for selective target protein binding in *ex vivo* pathological and normal human tissues to establish biomarkers of patient responses. Such methods have the potential to improve outcome of clinical trials by eliminating sub-optimal candidate drugs already in preclinical research, and they could help select optimal targeted therapies in clinical routine[4,8].

Recent advances in drug development include the preparation and screening of large collections of DNA-barcoded compounds, also known as DNA-encoded chemical libraries (DECLs), permitting single-pot screens of oligonucleotide-modified compounds[37-41]. We hypothesized that it might be possible to use DNA-conjugated drugs as affinity reagents to visualize target engagement directly in human tissues. This is in analogy to our and others' use of molecular genetics tools in antibody-directed rolling circle amplification (RCA) reactions, and for *in situ* proximity ligation assays (isPLA) [42-45]. We describe herein this target engagement-mediated amplification (TEMA) method, and its application for investigating localized target and off-target engagement on protein arrays as well as in cells and tissues.

We established TEMA using clinically approved tyrosine kinase inhibitors (TKIs), modified by covalently attaching oligonucleotides. These DNA-conjugated drugs were allowed to interact with their targets in model systems of increasing complexity, moving from protein arrays to cultured cell preparations and then sections from patient tissue samples. The localization of each physical interaction was visualized by amplification of circularized oligonucleotide probes via RCA, generating localized amplification products for each bound drug molecule (Fig. 1a). In a variant of the technique, TEMA is combined with proximity ligation (proxTEMA) by applying the DNA-conjugated small molecules together with antibody-DNA conjugates to achieve molecular resolution in target engagement through isPLA. This form of the assay focuses the *in situ* analyses of drug binding to specific on- or off-target proteins in a sample. Besides revealing cellular target engagement in clinically relevant samples, DNA-conjugated drugs also significantly broaden the repertoire of affinity reagents for probing the presence and localization of proteins.

Results

Design and Synthesis of TEMA Probes. Experimental assessment of TEMA required suitable DNA-conjugated small molecule-based probes. For this purpose, we focused on tyrosine receptor kinases for which multiple drugs are approved. This choice was based on several criteria: (1) availability of x-ray crystal structures of receptor-drug complexes; (2) a good understanding of structure-activity relationships; (3) literature precedence for conjugated drug analogs with retained binding to the primary targets. Importantly, this includes representatives with dissociation rates (k_{off}) on the hour scale[46-48], such that extensive washing protocols can be employed as customary in immunofluorescence-based assays; (4) literature data on kinase selectivity; (5) In-house access to relevant clinical material and; (6) availability of affinity reagents and prior experience in our labs of generating similar tool compounds. It was also desirable to include compounds with different selectivity profiles, such that observations with TEMA could be cross-validated against reference data.

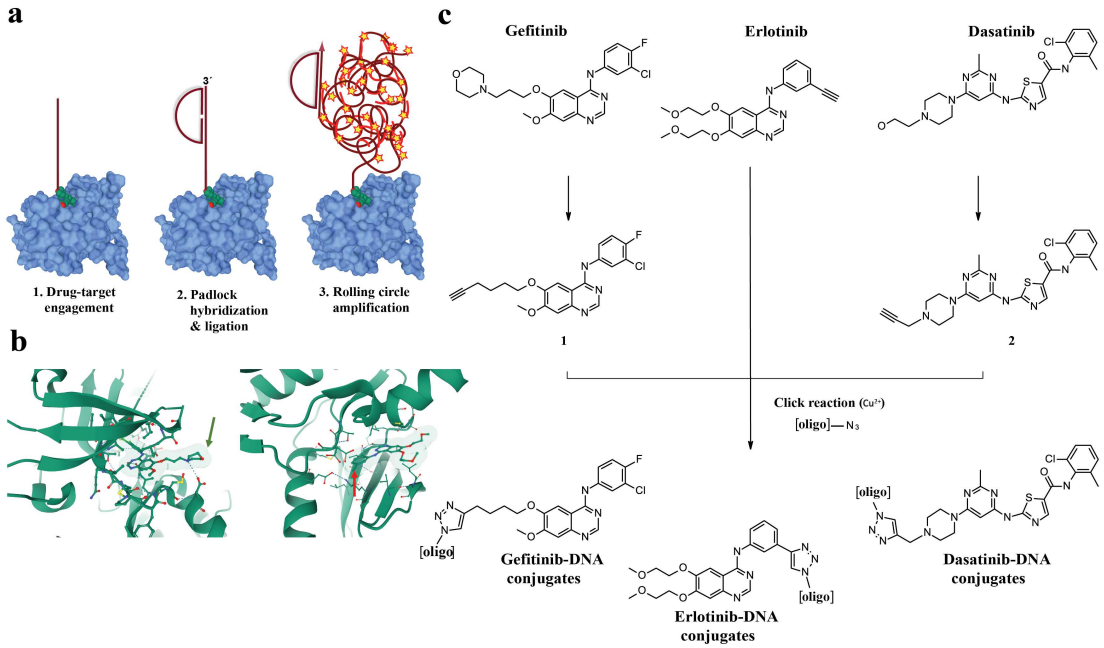

Fig. 1. Principle of TEMA and design of EGFR-directed drug-oligonucleotide conjugates. a, In TEMA, small molecule-based ligands conjugated to oligonucleotides bind their target proteins (1) in different sample matrices such as protein arrays, fixed cells and tissue sections. After washing away excess ligand, any remaining bound conjugate is recognized (2) by padlock probes[56]. These probes serve as substrates for ligation reactions and form DNA circles that template localized RCA reactions, the products of which are visualized using fluorescent oligonucleotide probes (3). The illustration of the EGFR kinase domain (light blue) is based on RSCB PDB (https://www.rcsb.org) entry 4WKQ (unpublished) using Mol*[57]. **b**, Illustration of binding by gefitinib (left) and erlotinib (right) in the active site of the EGFR kinase domain[55]. While the morpholine of gefitinib protrudes out of

the active site and represents a suitable exit vector for oligonucleotide conjugation (green arrow), the alkyne of erlotinib is buried in the active site such that conjugation causes steric hindrance (red arrow). The illustrations are based on RSCB PDB entries 4WKQ and 1M17 using Mol*. **c**, Structures of gefitinib, a selective EGFR-targeted drug, and dasatinib, with a broader kinase inhibition profile[17] (erlotinib was included as a control). The morpholines in gefitinib and dasatinib were replaced with an alkyne in precursors 1 and 2 and click chemistry afforded conjugation to azide-modified oligonucleotides. The corresponding alkyne precursors of gefitinib (1) and dasatinib (2) were synthesized and used to generate gefitinib- and dasatinib-DNA conjugates, respectively, while the alkyne in erlotinib allowed direct conjugation to provide erlotinib-DNA conjugates. Details on synthetic schemes and characterization of the molecules are available is Supplementary Information.

Given these considerations, we based our efforts on the specific epidermal growth factor receptor (EGFR) inhibitor gefitinib and the more promiscuous dasatinib, both of which have previously been modified at an exit vector protruding out of the active site of the target kinase[49-51]. Especially dasatinib dissociates slowly from its primary targets, with half-lives on the order of several hours. We utilized this information to introduce an alkyne moiety in parts of these molecules not involved in kinase interactions (Fig. 1b). Purified alkyne-containing drug analogs were further reacted with azide-labeled oligonucleotides using click chemistry to form triazole bonds between oligonucleotides and drugs[52-54]. Given the natural presence of an alkyne in erlotinib, a broader-spectrum EGFR drug, we included this as a control since direct conjugation to its alkyne is expected to hindrance active site binding in kinases[55]. The resulting drug-DNA conjugates were purified and quality checked prior to application in biological assays (Supplementary Figs. 1, 2 and Supplementary Information). As described in the next paragraph their suitability as affinity tools was verified by investigation of their binding profiles towards protein microarrays, including competition studies with unmodified drugs.

Application of TEMA on Protein Microarrays. Microarrays of displayed recombinant proteins represents a convenient format for fluorescent readout of discrete interactions, as previously demonstrated for DNA-conjugated antibodies following signal amplification via RCA[28-30]. Current literature include applications that also require functionality of the displayed proteins, such as their interactions with small molecules[58] and the identification of novel kinase substrates[58-60]. All proteins in the commercially available ProtoArray® Human Protein MicroArray (Thermo Fisher Scientific) have been purified and arrayed under native conditions to allow such studies. We adopted this format for investigation of the binding profiles of the drug-DNA conjugates. Circularizing oligonucleotides (padlock probes) were designed with 5' and 3' ends complementary to adjacent segments of the oligonucleotides conjugated to the drug molecules. Once converted to DNA circles by ligation, the probes could be replicated through localized RCA, primed by the drug-conjugated oligonucleotides, and visualized using fluorescence-labeled hybridization probes to the repeated sequence of the RCA products (Fig. 2a).

Using this approach both the dasatinib- and gefitinib-DNA conjugates were applied to planar arrays of >9,000 human proteins spotted in two technical replicates. The displayed proteins contain a glutathione S-transferase (GST) tag, allowing for control of levels of displayed protein using a fluorescence-labeled antibody that specifically recognizes GST with high affinity. Following incubation, washing, ligation, RCA amplification, and hybridization we recorded median fluorescence intensities (MFIs) for the spotted proteins, ranging from 25 to 64,992 arbitrary units for the dasatinib-DNA conjugate (Fig. 2c).

We observed prominent TEMA responses for a subset of ~100 proteins (Fig. 2b-c). A significant portion of those are relevant tyrosine kinases, with the strongest signals observed for known dasatinib targets such as Abl1, Abl2, Blk, Yes, Lyn, Src, PDGFRA and members of the ephrin receptor subfamily (Fig. 2b, -e). The hit list also contained a smaller number of protein phosphatases, with inosine monophosphatase 1 (IMPA1) and dual specificity protein phosphatase 14 (DUSP14) at the top of this list (Fig. 2b, d-e and Supporting Data 1).

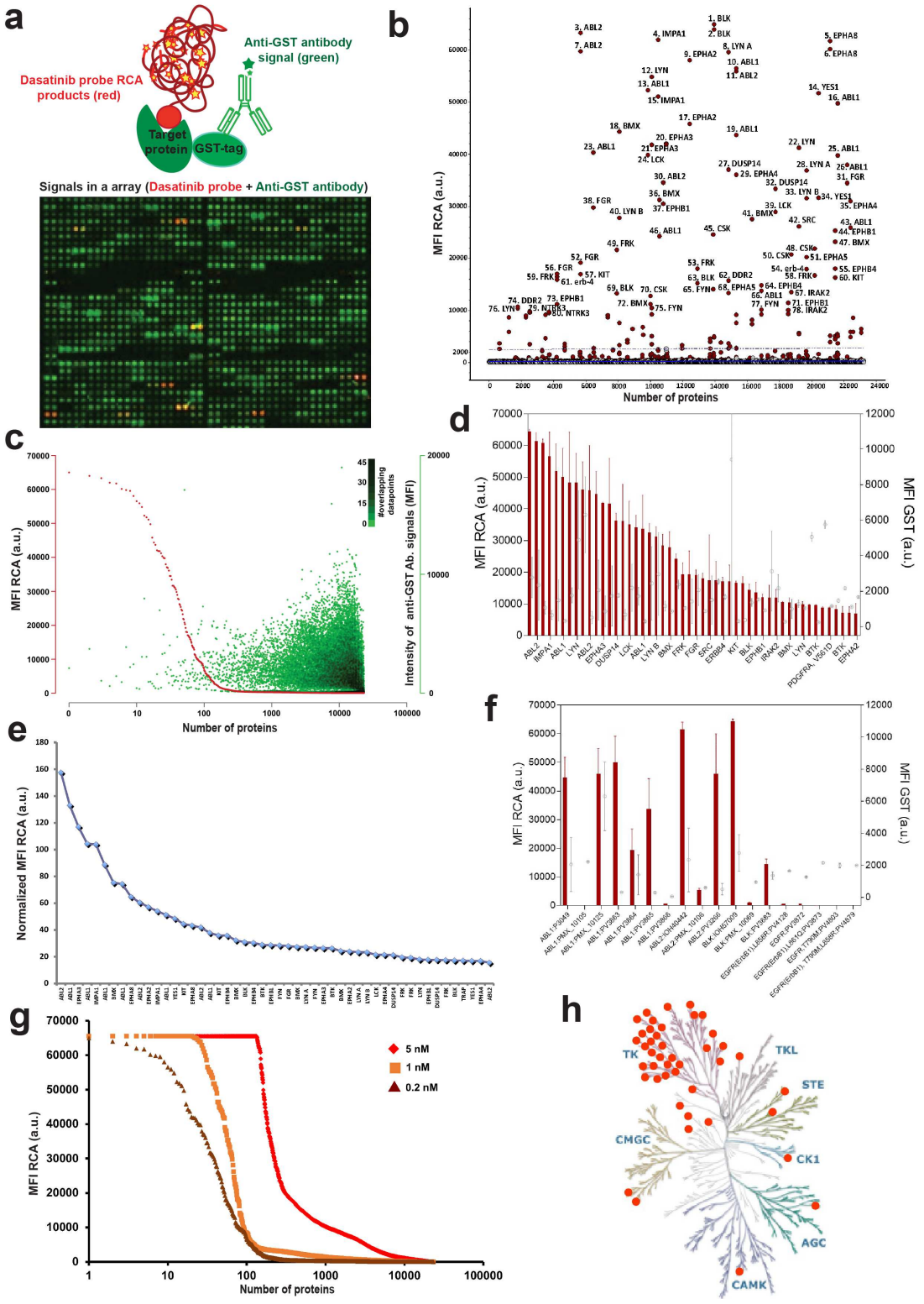

Fig. 2. **Array-based profiling of kinome specificity using TEMA. a**, Fluorescence signals from RCA products generated through binding of the dasatinib-DNA conjugates at 0.2 nM concentration to human proteins spotted in a microarray. Detection is achieved using a complementary oligonucleotide labeled with FarRed (red), while a Daylight 550-labeled antibody (green) directed against the GST tag was used to probe amounts of each spotted protein. **b,** Proteins as identified by TEMA for the dasatinib probe at 0.2 nM binding of each protein, the results illustrate signals from the 80 proteins yielding the highest values strong signals (>10,000 a.u.), almost all of them kinases as identified in the hits list. **c**, The median signals for the dasatinib probe (red) added at 0.2 nM was plotted on a log scale and in logarithmic order of decreasing intensity for the 9,000 proteins with replicates - in total 23,234

human protein spots. The signals from antibody-mediated detection of the GST tags of the same spotted proteins are plotted in green. **d,** MFI signals for the top 50 dasatinib hits (red bars; left y-axis) and the corresponding signals for GST (○; right y-axis) – error bars represent the difference between two technical replicates. **e**, Signals for the dasatinib probe at 0.2 nM binding to duplicate arrayed proteins as identified by TEMA, corrected for the amounts of each protein as determined by normalization of anti-GST antibody signals. The results illustrate signals for the 50 proteins yielding the highest values, almost all of them kinases as identified in the hits list. **f** MFI signals representing the TEMA and GST responses of the dasatinib probe for multiple variants of the same protein (same symbols and experimental conditions as in **b**). **g**, Investigation of the dasatinib target coverage by TEMA as a function of the concentration of the dasatinib conjugate – 0.2 nM (dark red line), 1 nM (orange line), and 5 nM (red line). **h**, Kinome dendrogram based on observed binding profiles of the dasatinib probe at 0.2 nM in arrays using TEMA with the cut-off signals above a 2,000 MFI threshold. The human kinome map dendrogram was adapted with permission from Cell Signaling Technology (www.cellsignal.com).

The observed kinase binding profile using TEMA is in broad agreement with published selectivity data for dasatinib[16-19] (Fig. 2h, Supplementary Figs. 6 and Supplementary Table 3), suggesting a significant portion of the arrayed proteins are functional. However, a small number of known dasatinib targets were missed (*e.g.* CSF1R, EPHB6, GAK, and MAP2K5) using a probe concentration of 0.2 nM. This prompted follow-up experiments at concentrations ranging between 0.2-5 nM (Fig. 2g), but these four kinases remained undetectable when tested with the dasatinib probe at 1 nM, and the experiment at 5 nM concentration did not yield a specific set of targets due to elevated background binding. The anticipated interactions with CSF1R and EPHB6 in the protein arrays, with reported sub-nM potencies[18], were thus missed across the TEMA experiments, while lack of signals for the low nM binders GAK and MAP2K5 could potentially be explained by the application of insufficient probe concentrations.

We undertook several experiments to understand the reason for the missed targets. First, we looked at the variability between technical replicates versus differences in response between different forms of the same kinase (included as separate products on the microarray). This is exemplified for top kinase hits in Figure 2b, d, where strong signals (>10,000 a.u.) were observed for five out of seven spotted variants of Abl1, while two of the spotted protein variants resulted in background signals only (this was true for both replicates of the two proteins). Similarly, for Abl2 and Blk two out of three variants showed positive responses (see Supplementary Fig. 5 for additional comparisons across the Ephrin receptor tyrosine kinases). These observations were not due to variation in amounts of spotted proteins, as significant GST signal were recorded for several of the inactive protein variants. Since EPHB6, GAK, and MAP2K5 were each only present once in the microarray, and CSF1R twice, we conclude that the lack of observed binding for the dasatinib probe may be because these proteins were non-functional.

Of particular note in this study was the lack of responses for all included forms of the EGFR receptor (Fig. 2f), demonstrating insufficient affinity of the dasatinib-DNA conjugate for retention on spotted EGFR variants during washes, possibly due to lack of functional proteins on the microarray. Reported affinities for dasatinib to different EGFR mutants range from the 20 nM and into the μM range[17-19], the application of the probe at 0.2 nM may therefore have been insufficient to allow retention of drug conjugates during the TEMA experimental procedure. Although a larger fraction of the proteins in the array exhibited detectable signals in follow-up experiments at 1 nM (Fig. 2g), none corresponded to the spotted EGFR proteins. Experiments were also performed at 5 nM probe concentration, resulting in significantly higher background binding but none of the EGFR products gave signals above a 10,000 MFI threshold (Supporting Data 1c). We conclude that although the manufacturer does not guarantee correct folding of proteins displayed on the arrays, the TEMA results show high intra- and inter-assay reproducibility and excellent agreement with results using other approaches for *in vitro* profiling of kinase inhibition.

In Situ TEMA Reveals Spatially Resolved Drug Binding in Cells and Tissues. For sufficiently specific probes, competition experiments can be extended to increasingly relevant model systems, *i.e.* going from isolated proteins and functional arrays to whole cells and

tissues[22,23]. The latter aspects are of particular interest as they allow analyses of patient material that are otherwise notoriously difficult to achieve.

Insight into the distribution of target binding drugs in cells and tissues can confer valuable information about the clinical potential of drug candidates. Having established by competition experiments that the DNA-conjugated variants of the TKIs retained strong and specific binding for their target proteins we sought to further examine this binding in situ in cells and tissues. We observed that levels of TEMA signals for five cell lines correlated well to their EGFR RNA expression as documented in the Human Protein Atlas (HPA, www.proteinatlas.org) RNA-seq cell line dataset; A431: 337.7, HaCAT: 229.9, SK-BR-3: 47.8, MCF-7: 3.1 $_{p}$TPM (Transcripts Per Million) and CHO-K1[48], and as investigated for protein expression by immunoblotting using two different EGFR-specific antibodies (Supplementary Fig. 7). HaCAT cells, grown in microtiter wells, were fixed and treated with variable concentrations of dasatinib probes, followed by detection via RCA. The numbers of RCA signals per cell were recorded by automated high-throughput image acquisition microscopy and image analysis using CellProfiler software (www.cellprofiler.org). Dasatinib probes at 100 pM generated strong, easily detectable fluorescent RCA products, while signals reached saturated levels at 10 nM concentrations (Supplementary Fig. 8). Using the gefitinib probe we observed that the DNA-conjugates at 5 nM generated strong localized fluorescence signals, representing interactions with target molecules in A431 cells that express high levels of the targeted EGFR protein (Fig. 3a). By contrast Chinese hamster ovary (CHO-K1) cells, serving as a negative control in the assay, failed to display significant signals, consistent with their lack of expression of EGFR[48] (Fig. 3a). The oligonucleotide-conjugated form of the narrow-spectrum clinical kinase inhibitor gefitinib generated significantly more signals in A431 cells, overexpressing the primary target EGFR, compared to K562 cells and the human macrophage cell line U937, where only few signals were observed (Fig. 3b). These results are consistent with the HPA RNA-seq dataset for K562: 0.0 and U937: 0.1 TPM, reflecting no or only very low expression of mRNA for the EGFR receptor in those cell lines. In contrast, the broad-spectrum clinical kinase inhibitor dasatinib exhibited higher signal intensity in the cancer cell line K562 overexpressing ABL along with other known target proteins for this drug (Fig. 3b). Additionally, we compared the distribution of binding by the dasatinib and gefitinib probes in SK-BR-3 cells by labeling their RCA products with two distinct fluorophores, revealing a preferentially perinuclear staining by the gefitinib probe but broader signal distribution by the dasatinib probe (Supplementary Fig. 9). The experiment illustrates the possibility to explore drug binding at subcellular resolution by TEMA.

We also used the drug-DNA conjugates to investigate the localization of drug binding in formalin-fixed healthy human colon tissue, expressing quite low EGFR levels, and in fresh-frozen breast cancer tissue. Strong dasatinib binding was observed in parts of the colon tissue, while gefitinib produced weaker staining (Fig. 3c). In breast cancer tissue the gefitinib probe specifically localized in tumor-containing parts of the sections, thus revealing the site of drug binding in this clinical material (Fig. 3d). An inactive probe, based on the kinase inhibitor erlotinib and serving as a control, was prepared by conjugating DNA to a region of the molecule known to engage in protein kinase targets binding. As expected, this nonfunctional probe resulted in weak to nonexistent staining in breast cancer tissue (Fig. 3d). The gefitinib probe gave stronger detection signals in formalin fixed gliosarcoma and glioblastoma tissue microarray samples compared to other investigated cancer tissues, while normal brain tissue exhibited only very few signals (Fig. 3e and Supplementary Fig. 10). The TEMA findings lend support to earlier studies suggesting that gefitinib-like model kinase inhibitors may be attractive candidate molecules to treat brain cancer patients[41-42]. We conclude that TEMA can generate *ex vivo* data revealing the distribution of drugs at cellular and subcellular resolution, as a basis for the evaluating their suitability as clinical drugs.

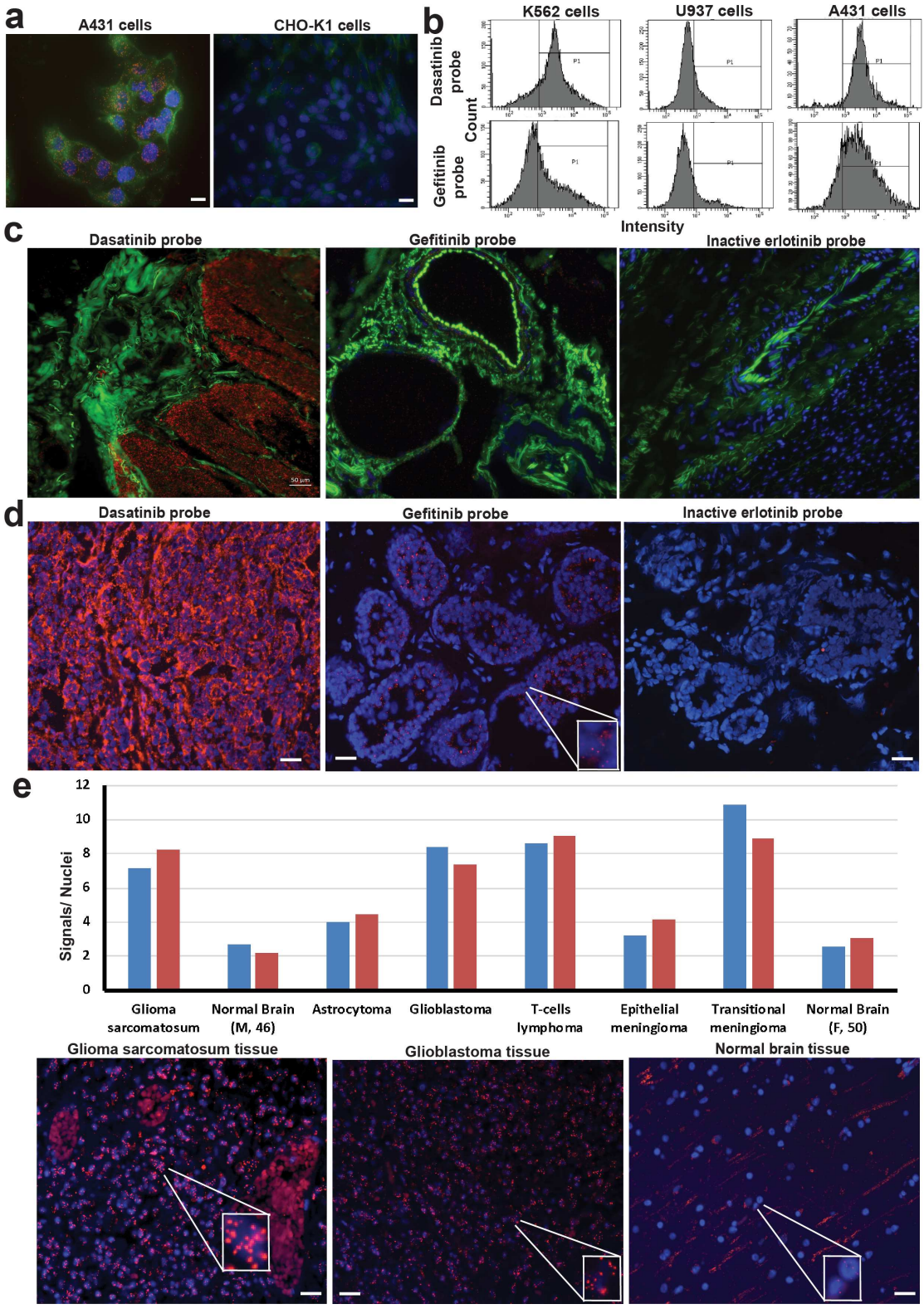

Fig. 3. Localization of drug binding in tissues by TEMA: a, Binding of gefitinib (at 5 nM; red dots) in the cancer cell line A431, expressing high levels of EGFR, and the CHO-K1 cell line, lacking expression of EGFR and used as biological control. Cytoplasms and nuclei were stained with phalloidin (green) and DAPI (blue), respectively. The images were acquired by fluorescence microscopy. Scale bars represent 20 µm. **b**, Flow cytometry analysis by TEMA for quantitative comparisons of target engagement by kinase inhibitor probes (5 nM) in K562 cells, overexpressing the ABL kinase as a fusion protein, and A431 cells, expressing EGFR transcripts at higher levels compared to U937 cells having low/absent EGFR expression. **c**, Comparison of binding by gefitinib and dasatinib probes at 1 nM in TEMA analyses of fresh-frozen normal human colon tissue sections. TEMA signals are seen in red, while nuclei in the

tissues were stained blue using DAPI. **d**, Investigation of fresh-frozen breast cancer tissue sections, previously scored as 3+ for HER2 protein staining by the HercepTest (Dako) , indicating high expression of HER2. TEMA probes at 1 nM signals are seen in red. **e**, Binding by gefitinib probes at 5 nM added to formalin-fixed paraffin-embedded brain cancer tissue sections and normal brain tissue in a commercial tissue microarray. The numbers of RCA products, representing TEMA gefitinib signals, were quantified per nuclei using CellProfiler software. The pairs of bars in distinct colors show duplicate observation for on average more than 2,000 cells in each sample type. RCA products are seen in red. Scale bars in panels (c), (d) and (e) are 50 μm.

Competition Experiments Against Unmodified Drugs. We explored the competitive mode for drug binding on arrays as well as in cells and tissues, demonstrating that signals could be reduced by competition both with unconjugated dasatinib drug molecules and with dasatinib molecules conjugated to oligonucleotides that themselves could not give rise to detection signals via RCA. We also performed competition experiments against a set of underivatized drugs with partly overlapping specificity to that of dasatinib. In analogy with other competitive binding formats[16,17,20,21], specific binding of TEMA probes to relevant kinases is expected to depend on the availability of active sites, where probes and drugs compete for binding. Thus, prior treatment with saturating concentrations of unmodified drugs or endogenous substrates should prevent probe binding. As expected, both dasatinib and staurosporine, with a broad kinase inhibition profile, completely blunted the RCA signal from the dasatinib probe when applied at equimolar concentrations (Fig. 4a). Bosutinib and ibrutinib also competed with the dasatinib probe, but complete competition was restricted to kinase targets for which their respective activities overlap with those of dasatinib[15-16,33-35], meaning significant responses were retained for BLK, KIT, DDR2, SRC, LCK, ABL1, ABL2, IMPA1, BMX, YES1, EPHB1 and PDGFRB also in the presence of equimolar concentrations of these inhibitors (see Supplementary Table 4 for a more complete comparison). These experiments demonstrate that protein microarray-based TEMA allows qualitative assessment of specificity profiles of kinase drugs, while the variability in retained function across spotted proteins precludes a complete quantitative assessment. An important prerequisite for these studies is a sufficiently slow off-rate of derivatized drugs for their primary target proteins, such that the compounds are retained during the extensive washes in the protocol.

The label-free original compound decreased dasatinib probe signals in A431 cells by an order of magnitude when present at equimolar concentrations in the reaction, whereas signals as expected were decreased by around one half with dasatinib, conjugated to an irrelevant oligonucleotide of a similar size (Fig. 4b-d and Supplementary Fig. 11b). A ten-fold molar excess of unmodified dasatinib drug molecules greatly reduced staining by the dasatinib-DNA conjugate in pathological tissue sections (Fig. 4g). We also observed similar competitive inhibition of binding by the gefitinib probe at 5 nM concentration in A431 cells with equimolar unmodified gefitinib (Fig. 4f). The experiments illustrate that binding by the DNA-conjugated compounds qualitatively reflects the properties of the unmodified drugs.

Analysis of Specific Target Engagement via Proximity Ligation Assay (proxTEMA). The TEMA technique described so far reveals all instances of drug binding in cells, tissues and protein arrays, whether on- or off-targets. We decided to adapt the technique in order to focus on the characteristics of drug binding to particular target proteins in situ. For this purpose, we developed proxTEMA assays as a variant of *in situ* proximity ligation assays, previously applied for antibody-based protein detection[45]. We combined DNA-conjugated drug molecules with DNA-conjugated antibodies directed against a potential target protein of interest (Fig. 5a). In this form of the assay, proximal binding by DNA conjugates of drugs and of protein-specific antibodies is required to give rise to the DNA circles that serve to template for RCA. This approach focuses the analysis of drug binding to specific on- or off-targets according to the antibody used (Fig. 5a and Supplementary Fig. 12e).

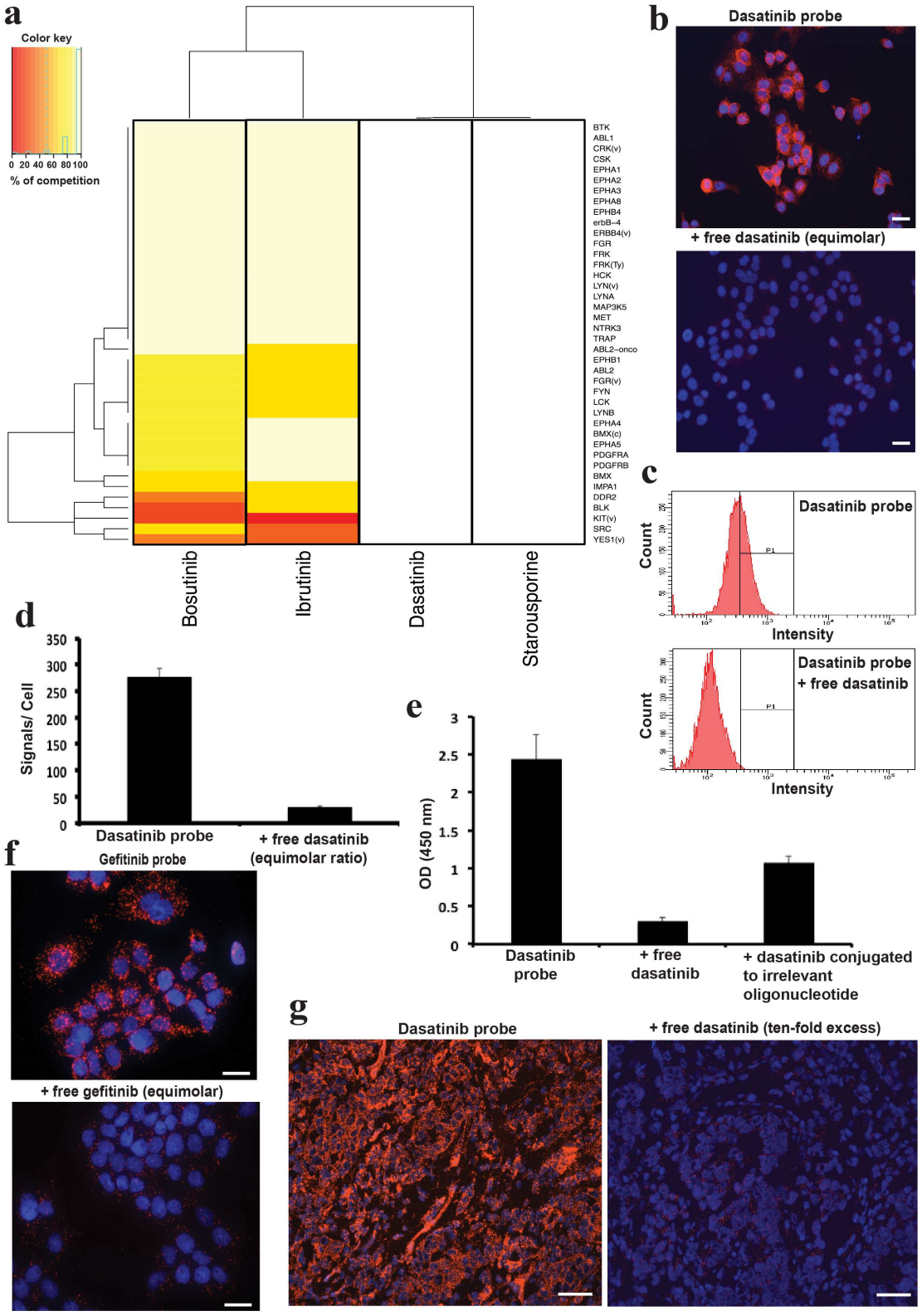

Fig. 4. Competitive TEMA on arrays, in cells and in tissue sections. a, Heat map illustrating competition between the dasatinib probe and four underivatized drugs on protein arrays. The dasatinib probe was added at 0.5 nM, alone or in competition with equimolar amounts of the unmodified kinase inhibitors dasatinib, staurosporine, bosutinib or ibrutinib. Dasatinib and staurosporine both completely inhibited binding by the dasatinib probe, while bosutinib and ibrutinib mainly inhibited binding to target proteins that are known to be shared with the dasatinib probe. The plot was generated using an in-house script developed in 'R'. Data represent means from two independents experiments). **b,** The dasatinib probe was applied at 1 nM to fixed MCF7 breast adenocarcinoma cells in the absence or presence of equimolar amounts of the unconjugated dasatinib drug, demonstrating strong

diminution of numbers of RCA products by this competition with the unmodified original compound. **c,** Flow cytometry readout of fixed A431 cells stained with a dasatinib probe applied at 10 nM alone or in competition with a 10-fold molar excess of unmodified dasatinib. The signals on the Y-axes reflect numbers of positive cells, while the fluorescence intensity per cell is indicated along the X-axes. Signals were recorded using a BD LSRII flow cytometer (in other experiments a BD Fortessa was used with similar results) with PE-Texas Red filter and the data were processed using BD FACSDiva software version 8.0. **d,** Competitive binding signals for the dasatinib probe at 1 nM in A431 squamous carcinoma cells by equal molar unlabeled dasatinib. The TEMA signals were quantified per nuclei using CellProfiler software and the bars show values for duplicate observation. **e,** A plot of total absorbance per well by colorimetric readout in cells using a microplate reader at wavelength 450 nm and absorbance at 650 nm as a reference. The bars show mean values of quadruplicate measurements with standard deviation (±). **f,** Competitive binding signals by the gefitinib probe at 5 nM in A431 cells in the presence or absence of the unmodified gefitinib drug. Scale bars, 50 μm. **g**, Competitive binding by the dasatinib probe in fresh-frozen breast cancer tissue with or without competition by a 10-fold molar excess of unmodified dasatinib.

As a proof-of-concept, we demonstrated specific interactions by dasatinib probes with the ABL kinase in BCR-ABL fusion protein positive K562 cells. We applied an oligonucleotide-conjugated anti-BCR antibody probe in combination either with anti-ABL kinase-specific antibody-oligonucleotide conjugate, or with the dasatinib probe as the pairs of affinity reagents, in both cases demonstrating the fusion proteins in K562 cells, with no signals in BCR-ABL fusion protein negative U937 cells (Fig. 5b, Supplementary 12e and Supplementary Fig. 12a). We further applied the proxTEMA approach by evaluating the specific binding of the gefitinib probe to the EGF receptor. The gefitinib probe was applied together with an oligonucleotide-conjugated anti-EGF receptor-specific antibody probe both in fixed A431 cells and in fresh-frozen breast cancer tissues scored as HER2 positive characterize it as grade+3 (Fig. 5c). The selectivity of the proxTEMA results were confirmed by analyses of EGFR negative CHO-K1 cells, and of normal human fresh-frozen colon tissue expressing very low EGFR levels as well as of breast cancer tissue section characterize it as a 0+ grade according to HER2 protein staining (Fig. 5c-d and Supplementary Fig. 12b-d). The results demonstrate that proxTEMA confers the unique ability to image drug binding to specific target proteins, directly in biological specimens.

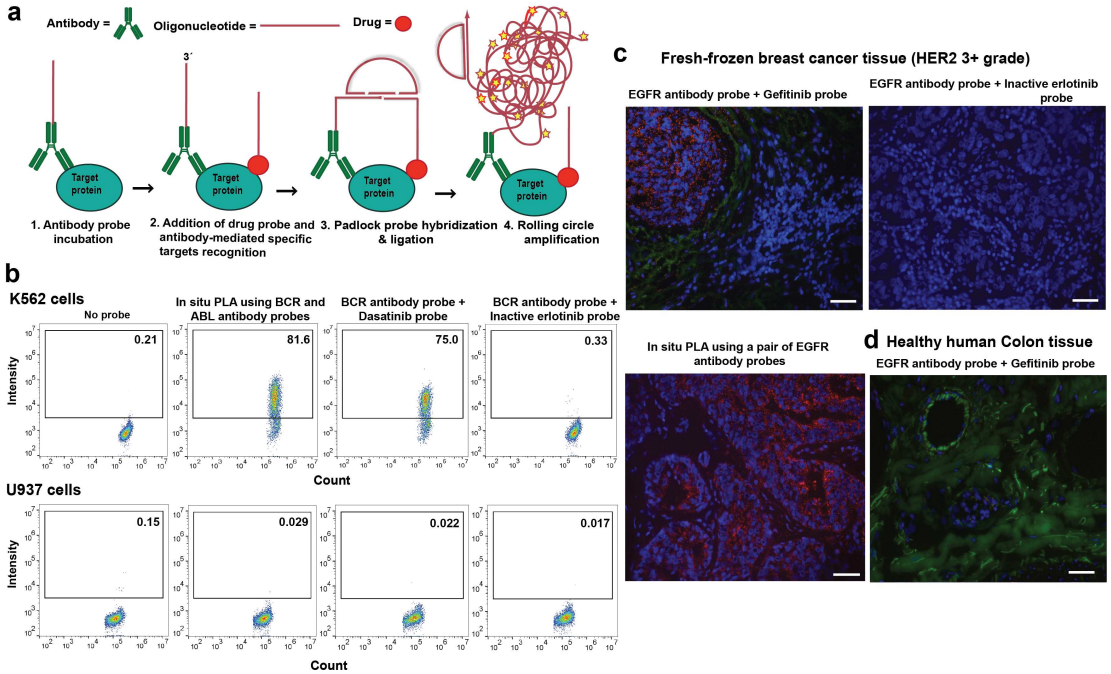

Fig. 5. Schematic of proxTEMA and application in cell lines and fresh frozen tissues sections. a, Using the ProxTEMA approach drug molecules with conjugated oligonucleotides were combined with oligonucleotide-conjugated antibodies directed against a protein of interest. In cases where both reagents bound the same or nearby target molecules their attached oligonucleotides could template the formation of DNA circles by ligating pairs of added oligonucleotides. Once formed the DNA circles were replicated in local RCA reactions, primed by oligonucleotides conjugated to the antibodies. **b**, ProxTEMA was used for detection of the BCR-ABL fusion proteins by flow cytometry using an anti-BCR antibody probe together either with an anti ABL antibody, or with either 2.5

nM of dasatinib or an inactive erlotinib reagent. The assays were performed in K562 cells, expressing this fusion protein, and in U937 cells that do express the fusion protein. The dasatinib probe can bind endogenous ABL proteins while the inactive erlotinib probe cannot. The experiment was repeated three times with similar results. **c**, Analysis of breast cancer sections by ProxTEMA using anti-EGFR antibody probes together with 10 nM gefitinib probes or inactive erlotinib probes. Signals are shown in red. For comparison a pair of EGFR-specific oligonucleotide-conjugated antibody probes were combined for isPLA to serve as a positive control. The breast cancer tissue sections had been scored as 3+ grade with respect to HER2 staining using a HercepTest (Dako). The tissues were counterstained using DAPI (blue) and images were acquired by fluorescence microscopy. Scale bar represents 50 µm. **d**, Demonstration of proxTEMA in normal human fresh-frozen colon tissue sections expressing low EGFR levels (green), negative control binding by 1 nM of gefitinib probe and EGFR specific antibody probe.

Discussion

Information about target engagement by drugs in relevant tissues is crucially important in the drug discovery process, and also in choosing the optimal therapy among growing numbers of alternatives in the clinic. We show that TEMA can reveal both specific and cross-reactive target engagement of drugs and drug candidates by applying the compounds with attached DNA strands. The approach enables highly sensitive and reliable visualization of the localization of binding of drugs to thousands of arrayed human proteins, in searches for compounds with specificity for particular target proteins, and with minimal cross reactivity for undesired target molecules. Another application of the TEMA technique allows high-content imaging with digital quantification in cell preparations and tissue sections. We demonstrate that the assays successfully recapitulate binding characteristics of the unmodified drugs. The assays afford excellent sensitivity, reproducibility and a potential for multiplexing. TEMA can help establish selectivity profiles and risks of toxicity, either by attaching an oligonucleotide to the drug candidate, or by investigating competition by unmodified drugs to a DNA-conjugated drug molecule for binding to a specific target site. We applied this competitive assay format herein to establish that drugs conjugated to irrelevant oligonucleotides exhibit qualitatively similar abilities to compete for binding to those of the unmodified drug molecules. We note that the drug dasatinib, central to our experiments, has a long residence time. Further experiments will be needed to see how TEMA will perform with reagents with faster off-rates. Nonetheless, we conclude that the DNA-drug conjugates investigated herein faithfully represent the properties of unmodified drugs albeit with some reduction of binding compared to the unmodified compounds.

Finally, by combining oligonucleotide-conjugated drugs with similarly modified antibodies, the *in situ* drug binding assays can be focused on targets of particular interest, using an isPLA mechanism. Assays similar to those described herein may prove suitable for analyses of e.g. broadly accessible fine needle biopsy material from tumor patients to establish the suitability of a given drug regime before therapy selection. In summary, TEMA represents a new approach to demonstrate target engagement by drugs in relevant biological material, suitable for application in the drug discovery process and with a potential for predicting patient responses to drugs.

Methods

Drug-DNA Conjugation by Click Chemistry. Copper-catalyzed click reactions of drugs containing alkyne group and azide-modified oligonucleotide were carried out using Invitrogen's buffer kit (catalog No. C10276). The reaction stoichiometry was optimized using the alkyne-containing drug molecules in molar excess (5-, 10-, 15-, 25-, 50- or 125-fold) over oligonucleotides. The reaction mixture contained 2X concentrated Click-iT® reaction buffer (component A), $CuSO_4$ (II) (component B, 100-fold molar excess over drug) in 100 µM reaction catalyst tris[(1-benzyl-1H-1,2,3triazol-4-yl)methyl]amine (TBTA, dissolved in DMSO). TBTA was added, followed immediately by the Click-iT® reaction buffer additive 1 (component C; should be colorless, discard brown solutions). The reaction components were mixed and incubated for 3 min at room temperature (RT). The reaction mixture solution turned bright orange upon addition of the final reaction buffer component D (click-iT® reaction buffer

additive 2 solution). The reactions were continued for an hour at RT and stopped by purification using Zeba™ Spin desalting columns (7k MWCO, Thermo Scientific). The DNA-conjugates were further purified using Slide-A-Lyzer Dialysis Cassette (3K MWCO, Thermo Scientific) over night at 4°C in phosphate buffered saline (PBS) to remove excess unreacted drug molecules. The conjugates were identified and pure probes were isolated through size exclusion chromatography using a Superdex 200 column in a HPLC system.

LC-MS Characterization. Starting materials (oligonucleotides and drugs), reaction component and conjugates were run in a BEH (Ethylene Bridged Hybrid Technology from Water) C18 1.7µm 2 x 50 mm column with the following mobile phases: (A) 400 mM hexafluoro-2-propanol, 10 mM triethylamine acetate pH 7 in 10% methanol and (B) 400 mM hexafluoro-2-propanol, 10 mM triethylamine acetate pH 7 in 90% methanol. The negative separation mode was applied in MS2 "Q1" ie "Q1 full scan mode" for full scan and MRM (Multiple Reaction Monitoring) with a general span of 200 Da. liquid chromatography was performed at a flow rate of 0.5 ml/min, with injection volume 7.5 µl, 80% A to 10% over 3 min in Waters XEVO TQ MS, coupled to an Acquity UPLC chromatographic instrument. All raw data were processed using the software Mass Lynx 4.1 (Waters Corp).

Surface Plasmon Resonance (SPR). A Biacore S51 SPR biosensor instrument (GE Healthcare) was used to characterize interactions between conjugates with known on- or off-target proteins. Human recombinant protein kinase ABL1 (Life Technologies) (20 µg/ml in 20 mM HEPES, pH 7.5) was immobilized directly on a CM5 biosensor chip surface by amine coupling, to a level of about 5000 RU. The running buffer contained: 50 mM Tris HCl pH 7.4, 150 mM NaCl, 10 mM $MgCl_2$, 1 mM $MnCl_2$, 0.005% Tween-20. A 1:1 serial dilution of drug conjugates was injected over immobilized ABL1 at concentrations ranging from 0.06 to 2 µM. All experiments were performed at a flow rate of 30 µl/min and at 25°C and data was analyzed using Biacore S51 Evaluation software (GE Healthcare).

Human Protein Microarray Experiments. ProtoArray® v5.1 (PAH05251020, ThermoFisher, Waltham, Mass), containing replicates of more than 9000 full length human proteins for a total 23232 spots per array. The proteins were expressed as N-terminal glutathione S-transferase (GST) fusions, expressed in using the Bac-to-Bac® Baculovirus Expression System available from Invitrogen and affinity purified under native conditions to retain their proper conformation. Oligonucleotide detection probes labeled with the fluorophore FarRed with emission wavelength similar to Alexa Fluor® 647 recommended for the reader, or antibodies conjugated with FITC, were used to detect RCA products and GST tag-specific anti-GST antibodies (DyLight® 550). The arrays were scanned using the CapitalBio LuxScan HT24) at two different wavelengths: F635 (red) for the FarRed detection probe and F635 (532) for the FITC-labeled detection probe or for anti-GST-conjugated DayLight® 550, serving to detect total protein amounts per spot. Data acquisition, alignment and image processing were performed using the GenePix® Pro microarray (v6.1) software. Statistical analysis of protein array data was based on log-transformed intensities and statistical software 'R'. The histogram was created using 'ggplot2 package R'.

Cell Preparation for TEMA. The cells were fixed in 3.7% paraformaldehyde on ice for 20 min and washed twice with DEPC-treated PBS, before being permeabilized with Tris-buffered saline with detergent (50 mM Tris-HCl, pH 7.5, 150 mM NaCl with 0.02% Triton) for 20 min. The cells were then washed twice with DEPC-treated PBS before TEMA experiments. For flow TEMA experiments, K562 and U937 cells were removed from the media by centrifugation and cell pellets were vortexted and washed once in 1xPBS, then fixed with 1% paraformaldehyde. A431 cells were trypsinized (0.25% trypsin/EDTA from Gibco) and then washed once in 1xPBS. All cells were fixed in 1% Formaldehyde Solution (Sigma Aldrich) in 1xPBS for 10 min on ice at RT. Cells were next pelleted to remove the fixation solution and washed in PBS. Permeabilization was performed by vigorous vortexing in 2 ml ice cold methanol (Sigma-Aldrich) and incubated for 10 min at 4°C, followed by two washes with 1xPBS + 1% BSA

(New England Biolabs, Boston, USA).

Fresh Frozen Tissue Specimen. Human fresh frozen, fully anonymized breast cancer tissue sections were obtained from the biobank at the unit for Clinical Pathology at Uppsala University Hospital, Sweden in accordance with Swedish biobank legislation (ethical approval is not needed for research on fully anonymized human tissue specimens according to the Swedish Ethical Review Act (2003:460)). Human normal frozen colon tissue from the Medical University of Graz, Austria were provided by the Biobank Graz with ethics approval of the project under the ethical commission number 23-015 ex 10/11, entitled 'Molecular and cellular characterization of colorectal cancer'. The tissue sections were stored at -80°C until fixation. The tissue sections were removed from storage at -80°C and fixed in ice-cold 3.7% formaldehyde for 20 min, and then permeabilized with TBS-0.02% Triton for 20 min. After permeabilization, the sections were washed twice in DEPC-treated PBS and immediately applied for experiments.

Tissue Microarrays. Formalin-fixed paraffin embedded brain tumor tissue array (T175a) including information about pathology grade and with normal brain tissue as controls, 12 cases/24 cores tissue specimens, were purchased from US Biomax. The tissue sections were prepared by deparaffinization through immersion in xylene for 20 min and then rehydrated in an ethanol series of 100%, 95% and 70% for 5 min each. Antigens were retrieved by pressure-cooking in Na-citrate buffer at pH 6.0 (10 mM sodium citrate, 0.05% Tween, 1xDAKO buffer diluted in water), washed with PBS and permeabilized with TBS-0.02% Triton for 20 min. After permeabilization, the tissue specimens were washed twice in DEPC-treated PBS and applied for in situ staining.

TEMA Experiments. All samples were incubated overnight at 4°C with blocking buffer containing 1 mg/ml BSA, 0.1 mg/ml salmon sperm DNA, 0.05% Tween20 in 1xTBS). Samples were quickly washed once with purified PBS and immediately incubated with drug probes (Supplementary Figure 2; probes 1a or 2a or 3a) and if required also with antibody probes for 60 min in PBS at 37°C, except for experiments where protein arrays were incubated with drug probes at RT. After incubation, samples were washed with TBS-Tween 20 (0.001%) for 1 min and a quick wash with hybridization and ligation buffer. Hybridization and ligation were performed with ligation buffer for 30 min at 37°C. The ligation buffer contained 10 mg/ml BSA, 10X T4 ligase buffer, 1mM ATP, 250 mM NaCl, 0.001% Tween20, 125 nM padlock probe oligonucleotides (5' phosphorylated PadlockP1-3, Supplementary Table 1) and 0.05 U/µL T4 DNA ligase in ddH_2O. Next, samples were washed with 1xTBS for 2x2 min and again quickly washed with RCA buffer, followed by RCA with 0.5 unit/µl Phi-29 DNA polymerase (Fermentas) in RCA buffer (1xPhi-29 DNA polymerase-buffer (Fermentas), 250 nM detection oligonucleotides (Detection tagD1, Supplementary Table 1), 7.5 nM polyA (Sigma-Aldrich), 0.25 µg/µl BSA, 0.25 mM dNTP (Thermo Scientific), 0.001% Tween in ddH_2O) incubated for 90 min at 37°C. The samples were washed twice with TBS-Tween 20 (0.05%) for 5 min, followed 1xTBS 2 x 5 min and quickly washed with purified water for 1 min at RT. Cells and tissues were stained with Alexa Fluor®488 phalloidin (1:50 in PBS- 0.01% BSA) and Hoechst dye (1:1000 in PBS- 0.01% BSA) both for 10 min at RT. For protein array experiments goat anti-GST antibodies (DayLight® 550) were diluted at 1:10,000 in PBS- 0.1% BSA and incubated for 60 min at RT.

TEMA with Flow Cytometry Readout. 1 x 10^6 cells were incubated for 45 min at 37°C in the Odyssey® Blocking Buffer in TBS containing 0.1% sodium azide (LI-COR Bioscience) after permeabilization and incubation. After centrifugation the blocking agent was decanted and the drug and antibody probes, diluted in PBS, were incubated with the cells for 90 min at 37°C. The cells were next washed with 1xTBS with 0.001% Tween 20 (Sigma-Aldrich), and incubated with 0.05 U/µl T4 DNA ligase in ligation buffer for the ligation step, followed by RCA. After one wash with TBS-0.01% Tween 20 the cells were placed in PBS and examined in a BD LSRII or BD Fortessa flow cytometer (BD Bioscience) using the PE-Texas Red filter.

The gating in the plots shows the fluorescence of the samples. Gating was performed by placing a gate around detected cells compared to a negative control incubated with the same azide-modified oligonucleotide without a conjugated drug molecule, using forward and side scatters. The positive events were detected using an antibody probe and gated cells were counted. The BD FACSDiva software version 8.0 (BD Bioscience) was used for data analysis.

ProxTEMA. All samples were incubated overnight at 4°C with blocking buffer containing 1 mg/ml BSA, 0.1 mg/ml salmon sperm DNA, 0.5% Tween 20 and 1xTris-buffered saline. The samples were washed with PBS for 1 min at RT and for the regular *in situ* PLA experiment conjugated anti-EGFR, anti-BCR and anti-ABL antibodies probes were diluted 1:100 in Duolink antibody diluent buffer (Sigma-Aldrich) and incubated for 1 hour at 37°C. For ProxTEMA, in a first step only the antibody probes (oligonucleotide-conjugated anti-EGFR, anti-BCR or anti-ABL), diluted 1:100 in Duolink antibody diluent buffer (Sigma-Aldrich), were incubated with the samples for 60 min at 37°C. After washes with TBS-Tween (0.01%) for 2x5 min, 2.5-10 nM DNA-conjugated drug probes (Supplementary Figure 2; probes 1b or 2b or 3b) were added and incubated for 90 min at 37°C in PBS, followed by washes with TBS-Tween (0.01%) for 2x2 min and then with ligation buffer for 1 min. Hybridization and ligation to generate circular reporter DNA strands were performed for 30 min at 37°C in ligation buffer containing 10 mg/ml BSA, 10xT4 DNA ligase buffer, 1 mM ATP, 250 mM NaCl, 0.05% Tween 20, 125 nM each of two phosphorylated oligonucleotides and 0.05 U/µl T4 DNA ligase in ddH_2O. The two oligonucleotides can be ligated to form a DNA circle, templated by the oligonucleotides conjugated to pairs of drug and antibody probes having bound in proximity (Fig. 6a and Supplementary Table 1). Samples were then washed with 1xTBS for 2x2 min and for one min in RCA buffer, followed by RCA for 90 min at 37°C with 0.5 unit/µl Phi-29 DNA polymerase (Fermentas) in RCA buffer. The samples were washed with TBS-Tween 20 (0.01%) for 2x5 min, in 1xTBS 2x5 min and quickly washed with purified water for 1 min at RT, protected from light.

Image Acquisition and Analysis. Images were acquired using an ImageXpress Micro automatic plate scanning microscope from Molecular Devices and an epifluorescence microscope (Zeiss Axioplan2 image station and Zeiss AxioCam camera MRm). For analysis in 96-well plates nine 20x magnification images were collected per well as low-resolution overviews of the 9 images in a 3x3 tile format using the MetaXpress software. CellProfiler software was used to analyze and quantify the images. Maximal intensity projection of the z-stacks was acquired using the CellProfiler cell image analysis software.

Online Content

Supporting Information: The Supporting Information is available on the website:

Correspondence Authors:

***Rasel A. Al-Amin:** orcid.org/0000-0002-0762-9034; E-mail: rasel.al-amin@igp.uu.se

***Ulf Landegren:** orcid.org/0000-0002-7820-1000; E-mail: ulf.landegren@igp.uu.se

Author Contributions: R.A.A., L.J., T.L., A.J.J. and U.L. conceived and designed the study. R.A.A. performed most of the experimental work. L.J. synthesized the precursor compounds; R.A.A. conjugated small molecules with DNA and analyzed results with M.H.. R.A.A., N.L. and U.L. designed and analyzed the protein array experiment. E.A. and R.A.A. performed SPR validation and analyzed with H.D.. R.A.A., R.S. and P.A. performed LC-MS/MS and analyzed the results. R.A.A., L.A., L.L., P.L. and A.B. cooperated on cell culture. R.A.A. and A.B. designed the tissue microarray experiment and R.A.A. performed the experiment. J.H. provided fresh frozen tissue. R.A.A. performed fresh frozen tissue experiment, A.B. and J.H. helped to analyze these. R.A.A., L.A. and L.L. performed flow cytometry experiments with advice from M.K.-M.. R.A.A. wrote a draft of the manuscript, U.L. and T.L. helped to edit it. All authors

contributed to the paper and have given approval to the final version of the manuscript.

Competing Interests

Ulf Landegren is a co-founder and shareholder of Navinci and Olink Proteomics, having rights to the PLA technology. Rasel A. Al-Amin and Ulf Landegren are co-founders and shareholders of PharmaPrecision AB.

Acknowledgements

We thank Drs. C.-M. Clausson and A. Klaesson for the kind help with the protocol for the fresh frozen breast tissue experiment and Prof. O. Söderberg for help analyzing these. Dr. A. Zieba Wicher assisted with deparaffinization of the tissue microarrays, Prof. P. Nilsson and the SciLifeLab autoimmunity profiling facility for assistance with the protein array experiments, and Prof. O. Kämpe for kindly providing materials used for the protein array experiments. This work was supported by a grant (2012-5852) from the Swedish Research Council's special call for future therapy, Swedish Research Council under grant agreement No. 2020-02258, a Torsten Söderbergs Stiftelse (M130/16) and the European Research Council under the European Union's Seventh Framework Programme (FP/2007-2013)/ ERC Grant Agreement No. 294409, ProteinSeq.

References

1. Morgan, P.; Van Der Graaf, P. H.; Arrowsmith, J.; Feltner, D. E.; Drummond, K. S.; Wegner, C. D.; Street, S. D. Can the flow of medicines be improved? Fundamental pharmacokinetic and pharmacological principles toward improving Phase II survival. *Drug Discov. Today* **17,** 419–424 (2012).
2. Bunnage, M. E.; Chekler, E. L.; Jones, L. H. Target validation using chemical probes. *Nat. Chem. Biol.* **9,** 195-199 (2013).
3. Cook, D.; Brown, D.; Alexander, R.; March, R.; Morgan, P.; Satterthwaite, G.; Pangalos, M. N. Lessons learned from the fate of AstraZeneca's drug pipeline: a five-dimensional framework. *Nat. Rev. Drug Discov.* **13,** 419-431 (2014).
4. Morgan, P.; Brown, D. G.; Lennard, S.; Anderton, M. J.; Barrett, J. C.; Eriksson, U.; Fidock, M.; Hamrén, B.; Johnson, A.; March, R. E.; Matcham, J.; Mettetal, J.; Nicholls, D. J.; Platz, S.; Rees, S.; Snowden, M. A.; Pangalos, M. N. Impact of a five-dimensional framework on R&D productivity at AstraZeneca. *Nat. Rev. Drug Discov.* **17,** 167-181 (2018).
5. Simon, G. M.; Niphakis, M. J.; Cravatt, B. F. Determining target engagement in living systems. *Nat. Chem. Biol.* **9,** 200-205 (2013).
6. Schurmann, M.; Janning, P.; Ziegler, S.; Waldmann, H. Small-molecule target engagement in cells. *Cell Chem. Biol.* **23,** 435-441 (2016).
7. Bowes, J.; Brown, A. J.; Hamon, J.; Jarolimek, W.; Sridhar, A.; Waldron, G.; Whitebread, S. Reducing safety-related drug attrition: the use of in vitro pharmacological profiling. *Nat. Rev. Drug Discov.* **11,** 909-922 (2012).
8. Bowes, J.; Brown, A. J.; Hamon, J.; Jarolimek, W.; Sridhar, A.; Waldron, G.; Whitebread, S. An analysis of the attrition of drug candidates from four major pharmaceutical companies. *Nat. Rev. Drug Discov.* **14,** 475-486 (2015).
9. Manning, G.; Whyte, D. B.; Martinez, R.; Hunter, T.; Sudarsanam, S. The protein kinase complement of the human genome. *Science* **298,** 1912-1934 (2002).
10. Hopkins, A. L.; Groom, C. R. The druggable genome. *Nat. Rev. Drug Discov.* **1,** 727-730 (2002).
11. Klaeger, S.; Heinzlmeir, S.; Wilhelm, M.; Polzer, H.; Vick, B.; Koenig, P. A.; Reinecke, M.; Ruprecht, B.; Petzoldt, S.; Meng, C.; Zecha, J.; Reiter, K.; Qiao, H.; Helm, D.; Koch, H.; Schoof, M.; Canevari, G.; Casale, E.; Depaolini, S. R.; Feuchtinger, A.; Wu Z.; Schmidt T.; Rueckert, L.; Becker, W.; Huenges, J.; Garz, A.K.; Gohlke, B.O.; Zolg, D.P.; Kayser, G.;

Vooder, T.; Preissner, R.; Hahne, H.; Tõnisson, N.; Kramer, K.; Götze, K.; Bassermann, F.; Schlegl, J.; Ehrlich, H.C.; Aiche, S.; Walch, A.; Greif, P.A.; Schneider, S.; Felder, E.R.; Ruland, J.; Médard, G.; Jeremias, I.; Spiekermann, K.; Kuster, B. The target landscape of clinical kinase drugs. *Science* **358***,* 4368 (2017).
12. Zhang, J.; Yang, P. L.; Gray, N. S. Targeting cancer with small molecule kinase inhibitors. *Nat. Rev. Cancer* **9,** 28-39 (2009).
13. Ferguson, F. M.; Gray, N. S. Kinase inhibitors: the road ahead. *Nat. Rev. Drug Discov.* **17,** 353-377 (2018).
14. Smyth, L. A.; Collins, I. Measuring and interpreting the selectivity of protein kinase inhibitors. *J. Chem. Biol.* **2,** 131-151 (2009).
15. Ghoreschi, K.; Laurence, A.; O'Shea, J. J. Selectivity and therapeutic inhibition of kinases: to be or not to be? *Nat. Immunol.* **10,** 356-360 (2009).
16. Fabian, M. A.; Biggs, W. H.; 3rd, Treiber, D. K.; Atteridge, C. E.; Azimioara, M. D.; Benedetti, M. G.; Carter, T. A.; Ciceri, P.; Edeen, P. T.; Floyd, M.; Ford, J. M.; Galvin, M.; Gerlach, J. L.; Grotzfeld, R. M.; Herrgard, S.; Insko, D. E.; Insko, M. A.; Lai, A. G.; Lélias, J. M.; Mehta, S. A.; … Lockhart, D. J. A small molecule-kinase interaction map for clinical kinase inhibitors. *Nat. Biotechnol.* **23,** 329-336 (2005).
17. Karaman, M. W.; Herrgard, S.; Treiber, D. K.; Gallant, P.; Atteridge, C. E.; Campbell, B. T.; Chan, K. W.; Ciceri, P.; Davis, M. I.; Edeen, P. T.; Faraoni, R.; Floyd, M.; Hunt, J. P.; Lockhart, D. J.; Milanov, Z. V.; Morrison, M. J.; Pallares, G.; Patel, H. K.; Pritchard, S.; Wodicka, L. M.; Zarrinkar, P. P. A quantitative analysis of kinase inhibitor selectivity. *Nat. Biotechnol.* **26***,* 127–132 (2008).
18. Davis, M. I.; Hunt, J. P.; Herrgard, S.; Ciceri, P.; Wodicka, L. M.; Pallares, G.; Hocker, M.; Treiber, D. K.; Zarrinkar, P. P. Comprehensive analysis of kinase inhibitor selectivity. *Nat. Biotechnol.* **29,** 1046-1051 (2011).
19. Anastassiadis, T.; Deacon, S. W.; Devarajan, K.; Ma, H.; Peterson, J. R. Comprehensive assay of kinase catalytic activity reveals features of kinase inhibitor selectivity. *Nat. Biotechnol.* **29,** 1039–1045 (2011).
20. Vasta, J. D.; Corona, C. R.; Wilkinson, J.; Zimprich, C. A.; Hartnett, J. R.; Ingold, M. R.; Zimmerman, K.; Machleidt, T.; Kirkland, T. A.; Huwiler, K. G.; Ohana, R. F.; Slater, M.; Otto, P.; Cong, M.; Wells, C. I.; Berger, B. T.; Hanke, T.; Glas, C.; Ding, K.; Drewry, D. H.; … Robers, M. B. Quantitative, wide-spectrum kinase profiling in live cells for assessing the effect of cellular ATP on target engagement. *Cell Chem. Biol.* **25,** 206–214 (2018).
21. Robers, M. B.; Vasta, J. D.; Corona, C. R.; Ohana, R. F.; Hurst, R.; Jhala, M. A.; Comess, K. M.; & Wood, K. V. Quantitative, real-time measurements of intracellular target engagement using energy transfer. *Methods Mol. Biol.* **1888,** 45-71 (2019).
22. Dubach, J. M.; Vinegoni, C.; Mazitschek, R.; Fumene Feruglio, P.; Cameron, L. A.; Weissleder, R. In vivo imaging of specific drug-target binding at subcellular resolution. *Nat. Commun.* **5,** 3946 (2014).
23. Dubach, J. M. et al. Quantitating drug-target engagement in single cells in vitro and in vivo. *Nat. Chem. Biol.* **13,** 168-173 (2017).
24. Dubach, J. M.; Kim, E.; Yang, K.; Cuccarese, M.; Giedt, R. J.; Meimetis, L. G.; Vinegoni, C.; Weissleder, R. In situ kinase profiling reveals functionally relevant properties of native kinases. *Chemistry & Biology* **18,** 699-710 (2011).
25. Patricelli, M. P.; Szardenings, A. K.; Liyanage, M.; Nomanbhoy, T. K.; Wu, M.; Weissig, H.; Aban, A.; Chun, D.; Tanner, S.; Kozarich, J. W. Functional interrogation of the kinome using nucleotide acyl phosphates. *Biochemistry* **46,** 350-358 (2007).
26. Cravatt, B. F.; Wright, A. T.; Kozarich, J. W. Activity-based protein profiling: from enzyme chemistry to proteomic chemistry. *Annu. Rev. Biochem.* **77,** 383-414 (2008).
27. Martinez Molina, D.; Jafari, R.; Ignatushchenko, M.; Seki, T.; Larsson, E. A.; Dan, C.; Sreekumar, L.; Cao, Y.; Nordlund, P. Monitoring drug target engagement in cells and tissues using the cellular thermal shift assay. *Science* **341,** 84–87 (2013).

28. Jafari, R.; Almqvist, H.; Axelsson, H.; Ignatushchenko, M.; Lundbäck, T.; Nordlund, P.; Martinez Molina, D. The cellular thermal shift assay for evaluating drug target interactions in cells. *Nat. Protoc.* **9,** 2100–2122 (2014).

29. Savitski, M. M.; Reinhard, F. B.; Franken, H.; Werner, T.; Savitski, M. F.; Eberhard, D.; Martinez Molina, D.; Jafari, R.; Dovega, R. B.; Klaeger, S.; Kuster, B.; Nordlund, P.; Bantscheff, M.; Drewes, G. Tracking cancer drugs in living cells by thermal profiling of the proteome. *Science* **346,** 6205 (2014).

30. Al-Amin, R. A.; Gallant, C. J.; Muthelo, P. M.; Landegren, U. Sensitive measurement of drug-target engagement by a cellular thermal shift assay with multiplex proximity extension readout. *Anal. Chem.* **93,** 10999-11009 (2021).

31. Perrin, J.; Werner, T.; Kurzawa, N.; Rutkowska, A.; Childs, D. D.; Kalxdorf, M.; Poeckel, D.; Stonehouse, E.; Strohmer, K.; Heller, B.; Thomson, D. W.; Krause, J.; Becher, I.; Eberl, H. C.; Vappiani, J.; Sevin, D. C.; Rau, C. E.; Franken, H.; Huber, W.; Faelth-Savitski, M.; … Bergamini, G. Identifying drug targets in tissues and whole blood with thermal-shift profiling. *Nat. Biotechnol.* **38,** 303-308 (2020).

32. Langebäck, A.; Bacanu, S.; Laursen, H.; Mout, L.; Seki, T.; Erkens-Schulze, S.; Ramos, A. D.; Berggren, A.; Cao, Y.; Hartman, J.; van Weerden, W.; Bergh, J.; Nordlund, P.; Lööf, S. CETSA-based target engagement of taxanes as biomarkers for efficacy and resistance. *Sci. Rep.* **9,** 19384 (2019).

33. Axelsson, H.; Almqvist, H.; Otrocka, M.; Vallin, M.; Lundqvist, S.; Hansson, P.; Karlsson, U.; Lundbäck, T.; Seashore-Ludlow, B. In situ target engagement studies in adherent cells. *ACS Chem. Biol.* **13,** 942–950 (2018).

34. Massey, A. J. A high content, high throughput cellular thermal stability assay for measuring drug-target engagement in living cells. *PLoS One* **13,** e0195050 (2018).

35. Innis, R. B.; Cunningham, V. J.; Delforge, J.; Fujita, M.; Gjedde, A.; Gunn, R. N.; Holden, J.; Houle, S.; Huang, S. C.; Ichise, M.; Iida, H.; Ito, H.; Kimura, Y.; Koeppe, R. A.; Knudsen, G. M.; Knuuti, J.; Lammertsma, A. A.; Laruelle, M.; Logan, J.; Maguire, R. P.; … Carson, R. E. Consensus nomenclature for in vivo imaging of reversibly binding radioligands. *J. Cereb. Blood Flow Metab*. **27,** 1533-1539 (2007).

36. Alcobia, D. C.; Ziegler, A. I.; Kondrashov, A.; Comeo, E.; Mistry, S.; Kellam, B.; Chang, A.; Woolard, J.; Hill, S. J.; Sloan, E. K. Visualizing ligand binding to a GPCR in vivo using NanoBRET. *iScience* **6,** 280-288 (2018).

37. Melkko, S.; Dumelin, C. E.; Scheuermann, J.; Neri, D. Lead discovery by DNA-encoded chemical libraries. *Drug Discov. Today* **12,** 465-471 (2007).

38. Clark, M. A.; Acharya, R. A.; Arico-Muendel, C. C.; Belyanskaya, S. L.; Benjamin, D. R.; Carlson, N. R.; Centrella, P. A.; Chiu, C. H.; Creaser, S. P.; Cuozzo, J. W.; Davie, C. P.; Ding, Y.; Franklin, G. J.; Franzen, K. D.; Gefter, M. L.; Hale, S. P.; Hansen, N. J.; Israel, D. I.; Jiang, J.; Kavarana, M. J.; … Morgan, B. A. Design, synthesis and selection of DNA-encoded small-molecule libraries. *Nat. Chem. Biol.* **5,** 647-654 (2009).

39. Gura, T. DNA helps build molecular libraries for drug testing. *Science (New York, N.Y.)* **350,** 1139–1140 (2015).

40. Mullard, A. DNA tags help the hunt for drugs. *Nature* **530,** 367-369 (2016).

41. Goodnow, R. A.; Jr.; Dumelin, C. E.; Keefe, A. D. DNA-encoded chemistry: enabling the deeper sampling of chemical space. *Nat. Rev. Drug Discov.* **16,** 131-147 (2017).

42. Schweitzer, B.; Wiltshire, S.; Lambert, J.; O'Malley, S.; Kukanskis, K.; Zhu, Z.; Kingsmore, S. F.; Lizardi, P. M.; Ward, D. C. Immunoassays with rolling circle DNA amplification: A versatile platform for ultrasensitive antigen detection. *Proc. Natl. Acad Sci. U. S. A*. **97,** 10113-10119 (2000).

43. Nallur, G.; Luo, C.; Fang, L.; Cooley, S.; Dave, V.; Lambert, J.; Kukanskis, K.; Kingsmore, S.; Lasken, R.; Schweitzer, B. Signal amplification by rolling circle amplification on DNA microarrays. *Nucl Acids Res*. **29,** E118 (2001).

44. Schweitzer, B.; Roberts, S.; Grimwade, B.; Shao, W.; Wang, M.; Fu, Q.; Shu, Q.; Laroche, I.; Zhou, Z.; Tchernev, V. T.; Christiansen, J.; Velleca, M.; Kingsmore, S. F. Multiplexed protein profiling on microarrays by rolling-circle amplification. *Nat. Biotechnol.* **20,** 359-365 (2002).
45. Söderberg, O.; Gullberg, M.; Jarvius, M.; Ridderstråle, K.; Leuchowius, K. J.; Jarvius, J.; Wester, K.; Hydbring, P.; Bahram, F.; Larsson, L. G.; Landegren, U. Direct observation of individual endogenous protein complexes in situ by proximity ligation. *Nat. Methods* **3,** 995-1000 (2006).
46. Kitagawa, D.; Gouda, M.; Kirii, Y. Quick evaluation of kinase inhibitors by surface plasmon resonance using single-site specifically biotinylated kinases. *J. Biomol. Screen* **19,** 453-461(2014).
47. Kumar, M.; Lowery, R. G. A High-throughput method for measuring drug residence time using the transcreener ADP assay. *SLAS Discov.* **22,** 915-922 (2017).
48. Georgi, V.; Schiele, F.; Berger, B. T.; Steffen, A.; Marin Zapata, P. A.; Briem, H.; Menz, S.; Preusse, C.; Vasta, J. D.; Robers, M. B.; Brands, M.; Knapp, S.; Fernández-Montalván, A. Binding kinetics survey of the drugged kinome. *J. Am. Chem. Soc.* **140,** 15774-15782 (2018).

49. Somwar, R., Erdjument-Bromage, H.; Larsson, E.; Shum, D.; Lockwood, W. W.; Yang, G.; Sander, C.; Ouerfelli, O.; Tempst, P. J.; Djaballah, H.; Varmus, H. E. Superoxide dismutase 1 (SOD1) is a target for a small molecule identified in a screen for inhibitors of the growth of lung adenocarcinoma cell lines. *Proc. Natl. Acad. Sci. U. S. A.* **108,** 16375-16380 (2011).
50. Brehmer, D.; Greff, Z.; Godl, K.; Blencke, S.; Kurtenbach, A.; Weber, M.; Müller, S.; Klebl, B.; Cotten, M.; Kéri, G.; Wissing, J.; Daub, H. Cellular targets of gefitinib. *Cancer Res.* **65,** 379-382 (2005).
51. Li, Z., Hao, P., Li, L., Tan, C. Y., Cheng, X., Chen, G. Y., Sze, S. K., Shen, H. M., & Yao, S. Q. Design and synthesis of minimalist terminal alkyne-containing diazirine photo-crosslinkers and their incorporation into kinase inhibitors for cell- and tissue-based proteome profiling. *Angew. Chem. Int. Ed. Engl.* **52,** 8551-8556 (2013).
52. Kolb, H. C.; Finn, M. G.; Sharpless, K. B. Click chemistry: Diverse chemical function from a few good reactions. *Angew. Chem. Int. Ed. Engl.* **40,** 2004-2021 (2001).
53. Rostovtsev, V. V.; Green, L. G.; Fokin, V. V.; Sharpless, K. B. A Stepwise Huisgen Cycloaddition process: Copper(I)-catalyzed regioselective "ligation" of azides and terminal Aakynes. *Angew. Chem. Int. Ed. Engl.* **41,** 2596-2599 (2002).
54. Wang, Q.; Chan, T. R.; Hilgraf, R.; Fokin, V. V.; Sharpless, K. B.; Finn, M. G. Bioconjugation by copper(I)-catalyzed azide-alkyne [3 + 2] cycloaddition. *J. Am. Chem. Soc.* **125,** 3192-3193 (2003).
55. Stamos, J.; Sliwkowski, M. X.; Eigenbrot, C. Structure of the epidermal growth factor receptor kinase domain alone and in complex with a 4-anilinoquinazoline inhibitor. *J. Biol. Chem.* **277,** 46265-46272 (2002).
56. Nilsson, M., Malmgren, H., Samiotaki, M., Kwiatkowski, M., Chowdhary, B. P., Landegren, U. Padlock probes: circularizing oligonucleotides for localized DNA detection. *Science*. **265,** 2085-2088 (1994).
57. Sehnal, D.; Rose, A. S.; Kovca, J.; Burley, S. K.; Velankar, S. In Workshop on Molecular Graphics and Visual Analysis of Molecular Data (*eds J. Byška, M. Krone, & B. Sommer*), 29-33 (2018).
58. Hett, E. C.; Kyne, R. E.; Jr, Gopalsamy, A.; Tones, M. A.; Xu, H.; Thio, G. L.; Nolan, E.; Jones, L. H. Selectivity determination of a small molecule chemical probe using protein microarray and affinity capture techniques. *ACS Comb. Sci.* **18,** 611-615 (2016).
59. Ptacek, J.; Devgan, G.; Michaud, G.; Zhu, H.; Zhu, X.; Fasolo, J.; Guo, H.; Jona, G.; Breitkreutz, A.; Sopko, R.; McCartney, R. R.; Schmidt, M. C.; Rachidi, N.; Lee, S. J.; Mah, A. S.; Meng, L.; Stark, M. J.; Stern, D. F.; De Virgilio, C.; Tyers, M.; … Snyder, M. Global analysis of protein phosphorylation in yeast. *Nature* **438,** 679-684 (2005).
60. Meng, L.; Michaud, G. A.; Merkel, J. S.; Zhou, F.; Huang, J.; Mattoon, D. R.; Schweitzer, B. Protein kinase substrate identification on functional protein arrays. *BMC Biotechnol.* **8,** 22 (2008).

Supplementary Files

This is a list of supplementary files associated with this preprint. Click to download.

- SupplementaryInformationTEMA.pdf
- SupportingData1Dasatinibprobe5nM.xlsx
- SupportingData1Dasatinibprobe1nM.xlsx
- SupportingData1Dasatinibprobe0.2nM.xls